RSC Advances

Journal Name RSCPublishing

COMMUNICATION

Elevated rate capability of sulfur wrapped with thin rGO layers for lithium sulfur batteries

Cite this: DOI: 10.1039/x0xx00000x

Wook Ahn[a*], Dong Un Lee[a], Hoon Sub Song[b], Sun-Hwa Yeon[c], Kwang-Bum Kim[d*], *Zhongwei Chen*[a]

Received
Accepted

DOI: 10.1039/x0xx00000x

www.rsc.org/

Sulfur-rGO composite is prepared a facile solution method using carbon disulfide solvent as a cathode electrode material for lithium-sulfur batteries to investigate its electrochemical performance. The initial capacity of sulfur-rGO composite is 1385 mAh/g obtained at 0.1 C-rate with the excellent average capacity reduction ratio of 0.37% per cycle (from 10th to 100th cycles).

1. Introduction

Lithium–sulfur (Li–S) batteries have been reported as one of the highly promising rechargeable lithium batteries due to the high theoretical capacity (1675 mAh/g), high energy density (2600 Wh/kg), low cost, and natural abundance of sulfur.[1-3] However, only a limited number of applications have been considered for utilizing Li-S batteries due to the poor intrinsic conductivity of pristine sulfur resulting in low material utilization and poor rate capacity of sulfur cathode, and the dissolution of polysulfide in organic electrolyte resulting in limited cycle stability and high self-discharge.[4-6] In recent years, many sulfur-carbon composites using various carbon materials which perform in the range of 1100 ~ 1400 mAh/g such as carbon nanotubes, amorphous carbon, mesoporous carbon, hollow structured carbon materials, graphene have been studied as electrode materials for Li-S batteries to overcome these intrinsic problems.[7-12] As reported in the literature, chemically dispersing conducting carbon materials with active sulfur not only reinforces the overall electrical conductivity of the cathode, but also effectively prevents the dissolution of lithium polysulfide into the electrolyte.[13, 14] This in turn greatly improves the utilization of active sulfur during charge-discharge processes. To take this into our advantage, we incorporate graphene, a two-dimensional, one atom-thick nanosheets structure, as a substrate and electrical conductor which is known to have excellent surface area and electrical conductivity.[15-19] Graphene based sulfur composite which shows good durability and rate capability prepared by the sulfur melting method and various chemical reaction route still faces some critical issues.[2,12,20] As mentioned previously, the electrochemical properties of sulfur-graphene composite have been improved by using commercial graphene or synthesized graphene sheets. Despite the improvement, however, there has been no further investigation which emphasizes the quality of graphene sheet and the number of graphene layers affecting the performance of graphene wrapped sulfur or graphene-sulfur composite. Moreover, in the previous works, the sulfur wrapped with graphene and sulfur-graphene composite have shown low initial discharge capacity and rate capability.[2,20]

Herein, we have designed a unique active electrode material for Li-S battery through a strategic synthesis of graphene coated sulfur composite by using a simple solution method. It is known that rGO dispersed in carbon disulfide (CS_2) solution is mixed with sulfur dissolved in CS_2 solvent under sonication, and CS_2 can be evaporated subsequently.[21] The number of graphene layer is compared between synthesized sulfur-rGO composite and simple mixture of sulfur-rGO materials. We demonstrate significantly improved electrochemical capacity of as-prepared sulfur-rGO composite by including a thin layer of graphene as a cathode for lithium sulfur battery application.

2. Experimental

2.1. Preparation of sulfur-reduced graphene oxide composite

The carbon disulfide assisted sulfur-rGO composite was obtained as follows and the process is presented in Fig. S1. 0.8

g sulfur was added in 20 ml carbon disulfide and immediately dissolved, and 0.2 g rGO dried in vacuum oven for 24 hours was dispersed in another 20 ml carbon disulfide then sonicated for 2 hours to exfoliate the rGO

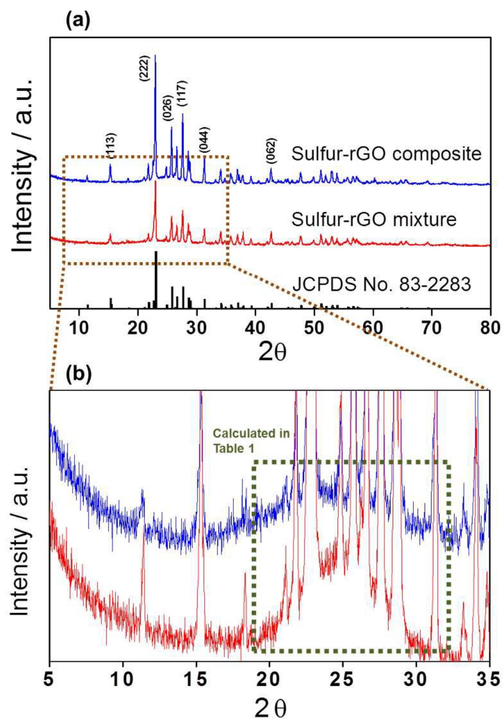

Fig. 1. The XRD patterns of sulfur-rGO composite, sulfur-rGO mixture (a); enlarged XRD patterns.for calculating the number of rGO layer in sulfur-rGO composite and sulfur-rGO mixture (b).

nanosheets. The sulfur dissolved solution was then gradually added to the rGO dispersed solution. Next, the mixed solution was sonicated for 2 hours then magnetically stirred at a medium speed and maintained at about 50 °C for 10 hours in a sealed bottle to suppress evaporation of carbon disulfide and create pressure for incorporation of sulfur into the wrinkles of rGO. Then, the solution was stirred to allow evaporation of carbon disulfide and recrystallization of sulfur. The black recrystallized sulfur-rGO composite was washed with ethanol and distilled water then dried in vacuum for 12 hr. In order to compare with the electrochemical properties, a simple mixture of sulfur and rGO was prepared using ball-milling method. To adjust the amount of sulfur in a simple mixture to sulfur-rGO composite, the slurry was manufactured as same component condition (60 wt.% of sulfur, 15 wt.% of rGO, 5 wt.% of conducting material and 20 wt.% of binder).

2.2. Characterization: physical and electrochemical properties

To confirm the amount of sulfur content in the sulfur-rGO composite, thermogravimetric analysis (TGA/SDTA851e-METTLER) was performed across a temperature range of 25 – 600 °C with a 5 °C min-1 heating rate in nitrogen atmosphere. For the structural analysis, X-ray diffraction of the phases was carried out using a HPC-2500 XRD (Gogaku) with Cu Kα radiation (λ = 1.5405Å) in the 2θ range of 10 – 80° with 0.02° intervals, at a 2°/min scanning rate. The morphology of the synthesized sulfur-rGO composite was analyzed using a scanning electron microscope (SEM; S4700, Hitachi). To prepare a cathode electrode for electrochemical testing, a composite powder of sulphur-rGO and acetylene black was mixed with PVdF-co-HFP

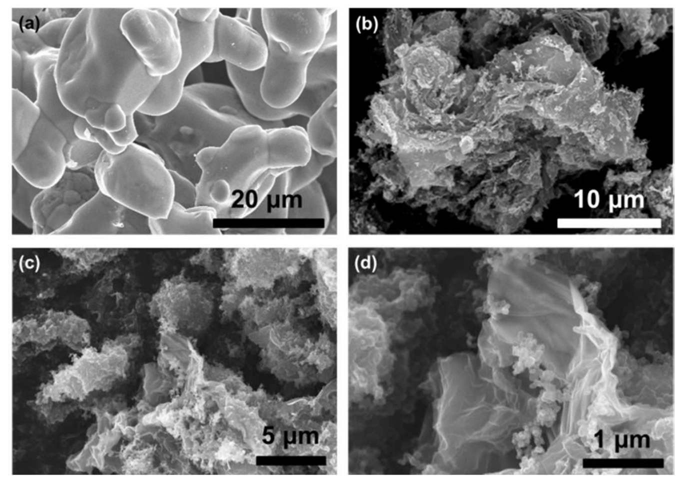

Fig. 2. SEM images of (a) pristine sulfur, (b) sulfur-rGO mixture and (c), (d) synthesized sulfur-rGO composite.

(Kynar 2801) in N- Methyl pyrrolidinone (NMP) solution. The composite electrode consisted of 75 wt.% sulfur-rGO, 5 wt.% conducting material and 20 wt.% binder. This slurry was then coated on an Al foil (20 μm) and finally dried under vacuum at 60 °C for 48 h. The electrode was subsequently pressed using a twin roller. The final thickness of the cathode material on the Al foil was 50 μm. In the present work, the sulfur-rGO composite electrode and the reference sulfur electrode mixed with rGO are denoted as the sulfur-rGO composite and sulfur-rGO mixture, respectively. Electrochemical experiments were performed in 1.0 M $LiCF_3SO_3$ and 0.2 M $LiNO_3$ in a mixture of tetra(ethylene glycol) dimethyl ether (TEGDME) / 1,3-dioxolane (DOL) (50:50 vol.%) using a coin-type cell(CR2032) with a Li counter electrode. The charge-discharge test was carried out with a Maccor series 4000 at 0.1 C-rate with a voltage range of 1.6 - 2.7 VLi/Li+. All of the specific capacity values in the present work were calculated on the basis of sulfur mass. Electrochemical impedance spectra were recorded by using a Zahner IM6 with application of an ac-amplitude of 5 mVrms on an open circuit potential over a frequency range from 105 Hz down to 10-2 Hz. All electrochemical experiments were carried out at room temperature.

3. Results and discussion

3.1. Structural features and physical properties

To confirm the sulfur quantity in the sulfur-rGO composite, the TGA analysis was performed from 25 °C to 600 °C under a nitrogen atmosphere as shown in Fig. S2. There are two weight loss stages apparent in the TGA curve. The first stage of abrupt weight loss in a ca. 25 °C – 350 °C temperature range reflects the sulfur decomposition and the weight loss is approximately 81 wt.%, in accordance with our previous work.[14]

Fig. 1 presents the XRD pattern of sulfur-rGO composite, which correspond to the orthorhombic phase with the space group Fddd (JCPDS 83-2283). Also, no peaks due to impurities have been found with the exception of slightly broaden XRD peaks around 26°. The slightly broaden peak is ascribed to the dispersed rGO, and sulfur-rGO composite was synthesized homogeneously by simple solution-based route. The XRD pattern of simply mixed reference sulfur-rGO

sample	(002) plane			
	FWHM	Lc (nm)	d-spacing (nm)	Number of layers
S-rGO mixture	9.26	3.5	0.41	8.5
S-rGO composite	18.46	1.8	0.40	4.5

Table 1. XRD results of sulfur-rGO mixture and sulfur-rGO composite including interlayer d-spacing (nm) and number of layers.

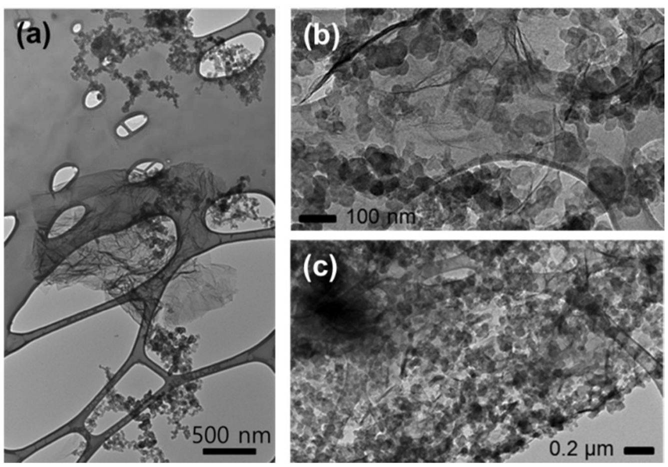

Fig. 3. TEM images of (a) sulfur-rGO mixture; (b) and (c) sulfur-rGO composite wrapped by thin rGO layers.

mixture also shows peaks that correspond to the orthorhombic phase with the broaden peaks at the same angles. However, the broaden peaks of sulfur-rGO mixture show relatively high intensity of rGO peak compare to that of sulfur-rGO composite, which is most likely due to different number of rGO layers. From this result, the number of layers of rGO in composite and mixture have been estimated. The number of layers was calculated from average crystallite (Lc) of the Scherrer–Debye Equation ($Lc = 0.89\lambda/\beta cos\theta$) and the number of layer for rGO has calculated as 4 layers in our previous work.[22] The number of rGO layers is found to be 4.5 in sulfur-rGO composite and 8.5 in sulfur-rGO mixture (Table 1). This result is an indication that the sulfur can be readily wrapped with thin layer of rGO sheets (under 4.5 layers) and coated on the surface of rGO using solution method. However, for the simple mixture of sulfur and rGO, the thin layer of rGO from starting material is re-stacked and agglomerated after ball milling procedure. The SEM and TEM images of synthesized rGO are presented in Fig. S3. These images reveal thin-layered and wrinkled rGO, which is morphologically highly suitable as high surface area electrical conductor for combining with active sulfur.

The morphology of sulfur-rGO composite and the employed pristine sulfur are presented in Fig. 2. The particle size of sulfur employed sulfur-rGO composite and mixture (a) shows about 5 ~ 10 µm, however, after composite synthesis where the sulfur particles dissolved in carbon disulfide and re-crystalized, nano-sized sulfur particles have formed on the surface of rGO. In addition, the nano-sized sulfur particles are well-dispersed and mixed homogeneously with the sheets of rGO creating an effective composite. However, sulfur and rGO is observed to be non-uniformly mixed in sulfur-rGO

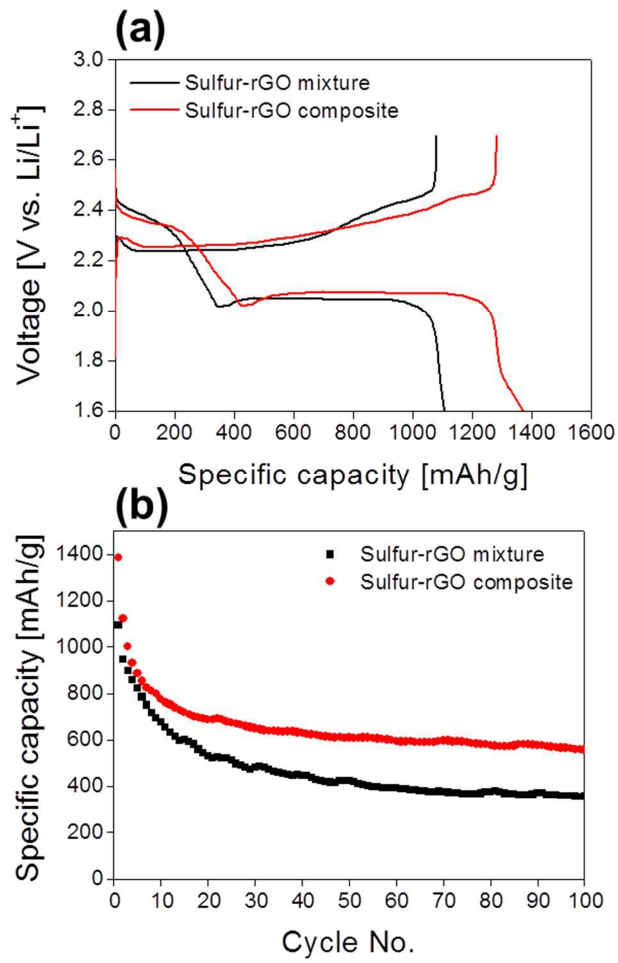

Fig. 4. (a) The comparison of initial charge-discharge profile of sulfur-rGO composite and sulfur-rGO mixture electrode, and (b) their cycleability.

mixture. It is noted that the precipitated sulfur could be easily form the nuclei of sulfur because the rGO still has functional groups in the inter-layer and on the surface of rGO. Therefore, the sulfur easily precipitated to the active sites of rGO, multiply.

Fig. 3 shows the TEM images of sulfur-rGO mixture (a) and sulfur-rGO composite wrapped with thin layer of rGO sheets ((b) and (c)), respectively. As seen in Fig. 3 (b) and (c), synthesized sulfur particle is homogeneous and uniformly dispersed with rGO. The primary particle size of sulfur is ca. 50~100 nm and the nano-sized sulfur particles are aggregated, forming huge sulfur particle. This huge sulfur particle, then, is wrapped with rGO sheets during the synthesis process. However, the sulfur-rGO mixture (Fig. 3 (a)) shows that the nano-sized (as-received) sulfur powders are not well dispersed. It is thus proposed that the sulfur in sulfur-rGO composite is synthesized as a nano-sized sulfur particle using solution method, and the synthesized sulfur is wrapped with rGO sheets including thin layer of rGO. On the other hand, it is verified that the rGO sheets separately existed with sulfur could be re-stacked during the mixing procedure, leading to the thick layer of rGO is mixed with sulfur particle. This result is in accordance with the number of rGO layers from XRD result.

3.2. Electrochemical properties

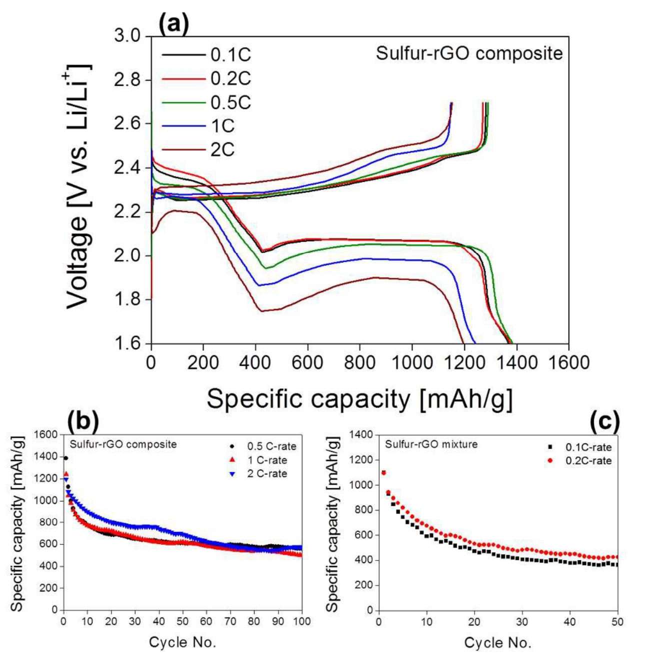

Fig. 5. Rate capability of (a) sulfur-rGO composite from 0.1 ~ 2 C-rate; (b) and (c) cycle performances of sulfur-rGO composite and sulfur-rGO mixture electrode at various C-rate.

The discharge-charge capacities and cycle performance have been evaluated to investigate the effect of graphene (rGO) on the electrochemical performance. Fig. 4 (a) and (b) display the comparison of typical discharge-charge profiles and cycle performances measured at a constant 167 mA/g (0.1 C-rate) based on the mass of sulfur, respectively, for both sulfur-rGO composite and mixture. Sulfur-rGO composite clearly delivers an excellent initial capacity of 1385 mAh/g, whereas the mixture has resulted in only 1090 mAh g-1 with the same amount of active material. In addition, sulfur-rGO composite shows higher capacity retention than the mixture after 100 cycles. The electrode prepared simple mixing procedure (sulfur-rGO mixture) shows larger particles; hence, the considerably reduced discharge capacities and abrupt decay in the cycle performances of those cathodes can be explained.

Fig. 5 (a) and (b) shows the rate capability and cyclability of sulfur-rGO composite at various applied C-rates. At applied C-rates of 0.1 and 0.2 C, virtually negligible capacity loss is observed between the two cells. From 0.5 to 2 C-rates, however, gradual over potential is observed resulting in capacity fading, however, the cell at 0.5 C-rate performed similar capacity compared with cell at 0.1 and 0.2 C-rate with showing over potential in discharge. Fig. 5 (c) shows the rate capability of sulfur-rGO mixture for 0.1 and 0.2 C-rates, where poor capacity retentions of 33 % at 0.1 C-rate and 38 % at 0.2 C-rate are observed, respectively, only after 50 cycles. The capacity reduction ratio per cycle is calculated and summarized in Table S1, where sulfur-rGO mixture shows high capacity reduction ratio within 40th cycle then drastically decrease with subsequence cycles being very stable. Moreover, the reduction ratio of the composite at 2 C-rate is even smaller than that of the mixture. From these results, significaltly enhanced electrochemical performance of sulfur-rGO composite as cathode material is highlighted in Li-S battery which is attributed to

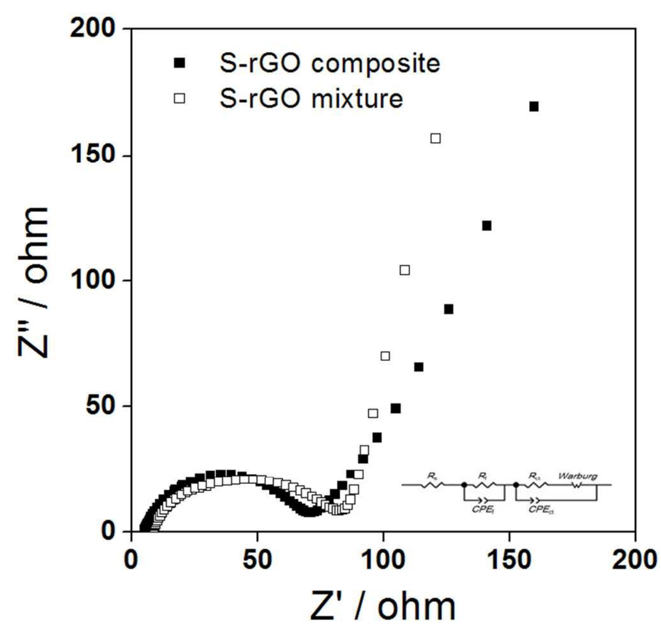

Fig. 6. Nyquist plots of the ac-impedance spectra measured on the cells obtained sulfur-rGO composite and sulfur-rGO mixture electrode.

the well-organized and uniformly distributed sulfur nanoparticles into the nanosheets of rGO as an effective composite for fast reaction kinetics.

Fig. 6 illustrate typical Nyquist plots of the ac-impedance spectra obtained from the Li-S cell with sulfur-rGO composite and sulfur-rGO mixture prior to cell testing. The measured ac-impedance spectra in the high frequency range and a straight line inclined at a constant angle to the real axis (Warburg impedance) in the low frequency are clearly present. In organic electrolyte, the sulfur transforms to soluble high-order lithium polysulfide, and thus the concentration of the dissolved lithium polysulfide in the electrolyte is related to the internal resistance. The increased concentration of the dissolved lithium polysulfide in the electrolyte strongly affects the viscosity of the electrolyte, resulting in a decrease of the electrolyte conductivity.[23] The electrolyte solution resistance (Rs) and charge- transfer resistance (Rct) are compared according to the equivalent circuit (inset). The Rs and Rct of sulfur-rGO composite and sulfur-rGO mixture are found to be 5.1, 71 Ω and 8.76, 82 Ω, respectively. As expected, both resistances of sulfur-rGO composite are lower than those of sulfur-rGO mixture. From this result, it could be attributed that well dispersed rGO is suppressing the penetration of soluble polysulfide into the organic electrolyte.

Conclusions

In summary, a homogeneous sulfur-rGO composite with well distributed sulfur nanoparticles is successfully synthesized by a facile solution impregnation method for lithium-sulfur batteries. From XRD and SEM results, the nano-sized sulfur particles are confirmed to be deposited on the surface or inter-layer of rGO. Sulfur-rGo composite comprises of sulfur nanoparticles with an orthorhombic phase and thin layers rGO nanosheets. When tested in lithium-sulfur cells, sulfur-rGO composite exhibits excellent performance with high specific capacity up to 1385 mAh/g at the initial discharge, and significantly improved cycle durability in compared to that of simple sulfur-rGO mixture. The rate capability of sulfur-rGO composite shows similar capacity within 0.5 C-rate and surprisingly even more stable capacity performance at 2 C-rate. From AC-impedance study, the interfacial resistance of sulfur-rGO composite is observed and homogeneously mixed rGO shows good electrochemical properties.

Notes and references

[a]Department of Chemical Engineering, University of Waterloo, 200 University Ave W. Waterloo, ON, N2L3G1, Canada
[b]Canmet Energy, Natural Resources Canada, 1 Hannel Drive, Ottawa, ON, K1A1M1, Canada
[c]Korea Institute of Energy Research, 152 Gajeong-ro, Yuseong-Gu, Daejeon, 305-343, Korea
[d]Department of Materials Science & Engineering, Yonsei University, 50 Yonsei-ro, Seodaemun-Gu, Seoul, 120-749, Korea

Electronic Supplementary Information (ESI) available: Schematic diagram for synthesis procedure of sulphur-rGO composite (Fig. S1); TGA (Fig. S2); SEM and TEM images of synthesized rGO sheets (Fig. S3); The comparison of capacity reduction ratio (Table S1). See DOI: 10.1039/c000000x/

1 X. Ji and L. F. Nazar, *Journal of Materials Chemistry*, 2010, **20**, 9821-9826.
2. H. Wang, Y. Yang, Y. Liang, J. T. Robinson, Y. Li, A. Jackson, Y. Cui and H. Dai, *Nano letters*, 2011, **11**, 2644-2647.
3. J. Schuster, G. He, B. Mandlmeier, T. Yim, K. T. Lee, T. Bein and L. F. Nazar, *Angewandte Chemie International Edition*, 2012, **51**, 3591-3595.
4. X. Ji and L. F. Nazar, *Journal of Materials Chemistry*, 2010, **20**, 9821-9826.
5. Y.-J. Choi, Y.-D. Chung, C.-Y. Baek, K.-W. Kim, H.-J. Ahn and J.-H. Ahn, *Journal of Power Sources*, 2008, **184**, 548-552.
6. J. Wang, S. Chew, Z. Zhao, S. Ashraf, D. Wexler, J. Chen, S. Ng, S. Chou and H. Liu, *Carbon*, 2008, **46**, 229-235.
7. G. Zhou, D.-W. Wang, F. Li, P.-X. Hou, L. Yin, C. Liu, G. Q. M. Lu, I. R. Gentle and H.-M. Cheng, *Energy Environ. Sci.*, 2012, **5**, 8901-8906.
8. X. Tao, X. Chen, Y. Xia, H. Huang, Y. Gan, R. Wu and F. Chen, *Journal of Materials Chemistry A*, 2013, **1**, 3295-3301.
9. G. Xu, B. Ding, L. Shen, P. Nie, J. Han and X. Zhang, *Journal of Materials Chemistry A*, 2013, **1**, 4490-4496.
10. G. Xu, B. Ding, P. Nie, L. Shen, J. Wang and X. Zhang, *Chemistry-A European Journal*, 2013, **19**, 12306-12312.
11. Y. Zhang, Y. Zhao, A. Konarov, D. Gosselink, H. G. Soboleski and P. Chen, *Journal of Power Sources*, 2013, **241**, 517-521.
12. H. Wu, Y. Huang, M. Zong, H. Fu and X. Sun, *Electrochimica Acta*, 2015, **163**, 24-31
13. C. Jia-Jia, J. Xin, S. Qiu-Jie, W. Chong, Z. Qian, Z. Ming-Sen and D. Quan-Feng, *Electrochimica Acta*, 2010, **55**, 8062-8066.
14. W. Ahn, K.-B. Kim, K.-N. Jung, K.-H. Shin and C.-S. Jin, *Journal of Power Sources*, 2012, **202**, 394-399.
15. K. Ziegler, *Phys. Rev. Lett.*, 1998, **80**, 3113-3116.
16. S. Y. Zhou, *Nature Phys.*, 2006, **2**, 595-599.
17. A. K. Geim and K. S. Novoselov, *Nature materials*, 2007, 6, 183-191.
18. A. K. Geim, science, 2009, **324**, 1530-1534.
19. X. Li, W. Cai, J. An, S. Kim, J. Nah, D. Yang, R. Piner, A. Velamakanni, I. Jung and E. Tutuc, *Science*, 2009, **324**, 1312-1314.
20. Y. Cao, X. Li, I. A. Aksay, J. Lemmon, Z. Nie, Z. Yang and J. Liu, *Phys. Chem. Chem. Phys.*, 2011, **13**, 7660-7665
21. J. G. Roof, *Society of petroleum engineers journal*, 1971, **11**, 272-276.
22. W. Ahn, H. S. Song, S.-H. Park, K.-B. Kim, K.-H. Shin, S. N. Lim and S.-H. Yeon, *Electrochimica Acta*, 2014, **132**, 172-179.
23. H.-S. Ryu, H.-J. Ahn, K.-W. Kim, J.-H. Ahn, K.-K. Cho, T.-H. Nam, J.-U. Kim and G.-B. Cho, *Journal of power sources*, 2006, **163**, 201-206.